

Spatial and temporal features of summer extreme temperature over China during 1960–2013

Lisuo Hu^{1,2} · Gang Huang^{1,3} · Xia Qu^{3,4}

Received: 19 August 2015 / Accepted: 21 January 2016 / Published online: 4 February 2016
© Springer-Verlag Wien 2016

Abstract Based on daily air temperature data from 772 stations in China, the present study uses absolute index and percentile index to investigate the spatial and temporal features of summer extreme temperature over China during the period 1960–2013. The analysis indicates that Xinjiang and south-eastern China are two major domains where extreme heat events frequently occur and that the number of heat day (NHD) and the frequency of heat wave (FHW) both show an increasing trend throughout the country except for Shandong and Henan provinces where a decreasing trend is identified. Although the two leading empirical orthogonal function (EOF) modes of the NHD and the FHW based on the absolute index and percentile index have differences, the time series of the first principal components (PC1) are consistent; PC1 depicts opposite trends from 1960 to late 1990s and during the late 1990s to 2013. According to the climatology and EOF modes, four sub-regions are chosen: Chuanyu, Huanghuai, Southeast, and Xinjiang area. The inter-decadal variation over the four sub-regions differs, but the NHD and the FHW significantly increase after the mid-1990s. Based on Mann-Kendall method, it is found that the NHD and the FHW over Chuanyu exhibited abrupt shifts in 1978 and 2000;

sudden shifts occurred in 1973 and 2000 over Huanghuai; an abrupt shift occurred over the Southeast area in 2003.

1 Introduction

Extreme temperature is a low-probability event but exerts great influences on social economy, agricultural production, people's lives, and property. In recent years, the extreme temperature has been attracting increasing attentions (Easterling et al. 2000; Meehl and Tebaldi 2004). For instance, extreme temperature events happened in Western Europe and Russia, respectively, in 2003 and 2010 (Luterbacher et al. 2004; Dole et al. 2011), leading to a serious damage of property. Extreme weather and climate events occurred frequently over China, for example, in the summer of 2003, 2006, 2007, and 2013 (Yang and Li 2005; Chen and Fan 2007; Chen and Fan 2008; Peng 2014). All of the events caused serious influences on agriculture, energy, and human health.

The Fourth Assessment Report of the Intergovernmental Panel on Climate Change indicated that the frequency and intensity of the most extreme weather and climate events presented an increasing trend in the twentieth century and may continue to increase in the twenty-first century (Solomon et al. 2007). The Fifth Assessment Report also analyzed the changes of extreme events (Hartmann et al. 2013). Under background of climate change, the intensity, scope, and occurrence frequency of extreme weather and climate events are likely to change (Wang et al. 2012; Rummukainen 2013).

Numerous studies show that the frequency of global heat wave has increased in the second half of the twentieth century (e.g., Easterling et al. 2000; Alexander et al. 2006). Manton et al. (2001) and Choi et al. (2009) found that the hot days and warm nights of most stations over Asia-Pacific region show an increasing tendency. Using global station-observed data, Frich

✉ Gang Huang
hg@mail.iap.ac.cn

¹ State Key Laboratory of Numerical Modeling for Atmospheric Sciences and Geophysical Fluid Dynamics, Institute of Atmospheric Physics, Chinese Academy of Sciences, Beijing 100029, China

² University of Chinese Academy of Sciences, Beijing 100049, China

³ Joint Center for Global Change Studies, Beijing 100875, China

⁴ Center for Monsoon System Research, Institute of Atmospheric Physics, Chinese Academy of Sciences, Beijing 100029, China

et al. (2002) found that the duration of heat wave over Southeast China was reduced in the second half of the twentieth century.

Due to the complex terrain and climate of China, the changes of extreme temperature over China exhibit spatial features. Average surface temperature increased by 1.1 °C over the past 50 years (Ren et al. 2005), resulting in the changes of extreme temperature events. Former researches indicated that extreme temperature had a weakening trend over China with even a decreasing trend in east and south China (Zhai and Ren 1997; Ren and Zhai 1998; Yan and Yang 2000; Zhai and Pan 2003; Tang et al. 2005; Zhang and Qian 2008; Zhang et al. 2008). Recent researches indicated that there is a consistent increasing tendency in China, especially in eastern China (except for east central China) (Ding et al. 2009; Wang et al. 2012; Zhou and Ren 2011; Xu et al. 2013; Sun et al. 2014).

In addition to the spatial features, change of extreme temperature exhibits obvious temporal features. Shi et al. (2009) found that the daily maximum temperature and extreme heat days over east China had an inter-decadal variation. Sun et al. (2011) suggested that the frequency of heat wave shows inter-decadal variability in the past 50 years, with an obvious increase throughout the country since 1990s, especially over northwest and east China. Qi and Wang (2012) indicated that extreme heat days exhibit an abrupt shift in the early 1990s over China.

Different researches show different spatial and temporal features of summer extreme temperature over China. This is mainly due to various choices of extreme temperature indices, target periods, and regions. Continuous extreme temperature events have great impacts on human society, but former researches focusing on the duration of extreme temperature are not adequate. The objective of this paper is to provide a comprehensive analysis of observed extreme temperature over China. Thus, we use absolute index and percentile index and adopt the definition of a heat wave from the former work (Ding et al. 2009) to analyze the spatial and temporal features of a heat day and heat wave over China during 1960–2013.

2 Data and methods

The dataset with daily temperature is collected and processed by the National Meteorological Information Center (NMIC) of the China Meteorological Administration (CMA). The temperatures were recorded according to the standard observation rules for China (CMA. 1979). The observed values are quality controlled using the NMIC conventional procedures, including the climatological limit check, the station or regional extremes check, the internal consistency check, the temporal and spatial consistency checks, etc. (Li et al. 2004; Li et al. 2009; Xu et al. 2013). The target months are June, July, and August (JJA). In this study, the year with no missing value is judged as

available. A station with no less than 50 available years during 1960–2013 is adopted in this analysis. Thus, we select 772 stations over China, and the distribution of 772 weather observation stations in China is shown in Fig. 1.

Present investigation uses absolute index and percentile index to characterize the extreme temperatures. CMA defines extreme temperature as daily maximum temperature more than 35 °C. Considering the regional differences of extreme temperature, we use the 90th percentile value of daily maximum temperature to define extreme temperature simultaneously. Daily maximum temperatures during 1960–1989 are ranked in an ascending order and then the 90th percentile is chosen from the order as the percentile threshold.

The day when daily maximum temperature exceeds the threshold is defined as a heat day. When the daily maximum temperature exceeds the threshold for three consecutive days or more, it is defined as a heat wave event. The present study emphatically analyzes the spatial and temporal features of the number of heat day (NHD) and the frequency of heat wave (FHW). The descriptions of two extreme temperature indices, heat day and heat wave, are showed in Table 1.

Linear regression, 9-year sliding average, and empirical orthogonal function (EOF) are used to analyze a long-term variation of the NHD and the FHW. Student's *t* test is used to examine the significance of linear regression. Mann-Kendall method and 11-year sliding *t*-test are applied to detect sudden shifts.

3 Results

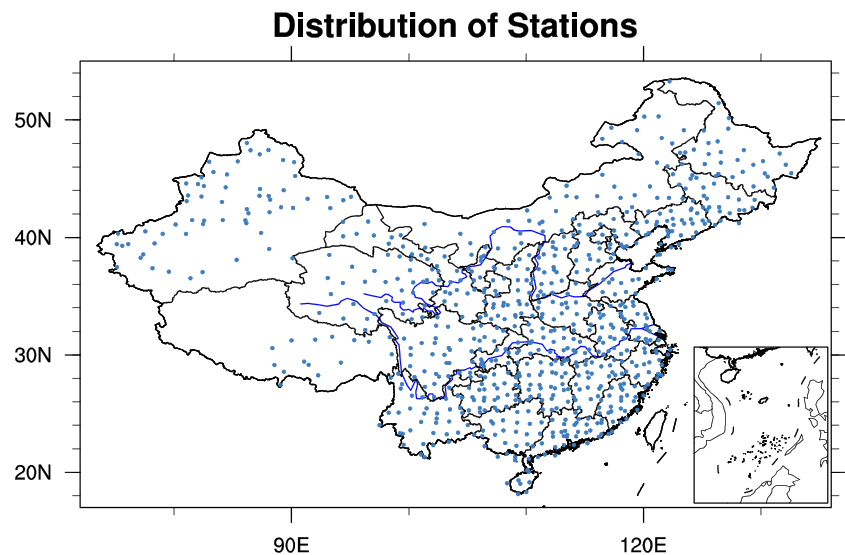
3.1 Climatology

Figure 2a shows climatology of the NHD based on absolute index over 772 weather observation stations in China during 1960–2013. The domains with frequent heat days mainly reside over Xinjiang, south of the Yangtze river, and Chuanyu area. The summer-averaged NHD increased gradually from northwest to southeast. A high-value center of the NHD is present in Xinjiang, which is due to long sunshine time and large covering areas of sand. One reason for high value of the NHD over south of the Yangtze river is the influence of the western Pacific subtropical high.

Figure 2b shows distribution of 90th percentile values of daily maximum temperature based on 1960–1989 over China. The low-value zones include the Tibetan Plateau, most of the northeast China, and Yunnan province. High value mainly located in Xinjiang, Huanghuai basin, and south of the Yangtze river. Compared with the high value areas of the NHD (Fig. 2a), distribution of the high value regions of 90th percentile is more extensive, especially in Huanghuai basin.

Figure 3a shows climatology of the FHW based on absolute index over 772 weather stations in China during 1960–

Fig. 1 Locations of 772 meteorological stations



2013. Major domains of the FHW reside over south Xinjiang and south of the Yangtze river. The FHW increases gradually from northwest to southeast. Figure 3b is the same as Fig. 3a but for the FHW based on percentile index. There is only one high-value center located in the south of the Yangtze river and low-value areas are observed in Shandong, Henan, and Yunnan province.

3.2 Long-term variation

3.2.1 EOF

The EOF analysis is applied to investigate the main spatial and temporal features of the NHD and the FHW of 772 stations over China during 1960–2013. Figure 4 displays the first two EOF modes and corresponding principal components for the NHD based on absolute index. The two modes explain about 38.4 % and 12.5 % of the total variances, respectively.

The first two principal components (PCs) for the NHD based on absolute index display inter-decadal variations (Fig. 4c, d). The EOF1 (Fig. 4a) features a positive anomaly covering northeast China and north of Xinjiang and a negative

anomaly covering most regions of China. The corresponding PC (Fig. 4c) depicts opposite trends during 1960 to the late 1990s and during late 1990s to 2013. The EOF1 and PC1 indicate that from 1960 to the late 1990s, the NHD increased over northeast China and north of Xinjiang, while it decreased over most regions of the China, especially in southeast China; the trends reversed in these areas during the late 1990s to 2013. The second EOF mode (EOF2, Fig. 4b) features a negative anomaly in south China and a positive anomaly over Huanghuai area and west Xinjiang. The corresponding PC (PC2, Fig. 4d) represents a decadal variation with 10a period. The EOF2 and PC2 revealed that the NHD increases (decreases) over Huanghuai area and west Xinjiang (south China) from the 1960s to 1970s and during the 1990s, and that the trends reversed in these areas during the 1980s and 2000s.

For the NHD based on percentile index, the first two EOF modes, are shown in Fig. 5, explain about 30.2 % and 14.7 % of the total variances. The first EOF mode (EOF1, Fig. 5a) features a consistent negative anomaly over China, and the first principal component (PC1, Fig. 5c) depicts opposite trends during 1960 to late 1990s and during the late 1990s to 2013. It indicates that the NHD based on percentile index decreased over China during 1960 to the late 1990s, especially in the Yangtze river basin, but increased during the late 1990s to 2013. The second mode (EOF2, Fig. 5b) shows a negative anomaly over north China (north of 35° N) and a positive anomaly over south China (south of 35° N). The corresponding PC (PC2, Fig. 5d) represents the opposite trends between 1960 and 1995 and 1995–2013. Thus, the NHD based on percentile index decreases in north China (north of 35° N) during 1960 to 1995, but increased in south China (south of 35° N). The trends reversed in these areas during 1995 to 2013.

The modes and PCs of the FHW based on two indices over China during 1960–2013 (figures are omitted) are consistent

Table 1 Descriptions of two indices, heat day and heat wave

	Description
Absolute index	35 °C
Percentile index	90th percentile value of daily maximum temperature during 1960–1989
Heat day	Daily maximum temperature exceed threshold
Heat wave	Daily maximum temperature exceed threshold for three consecutive days or more

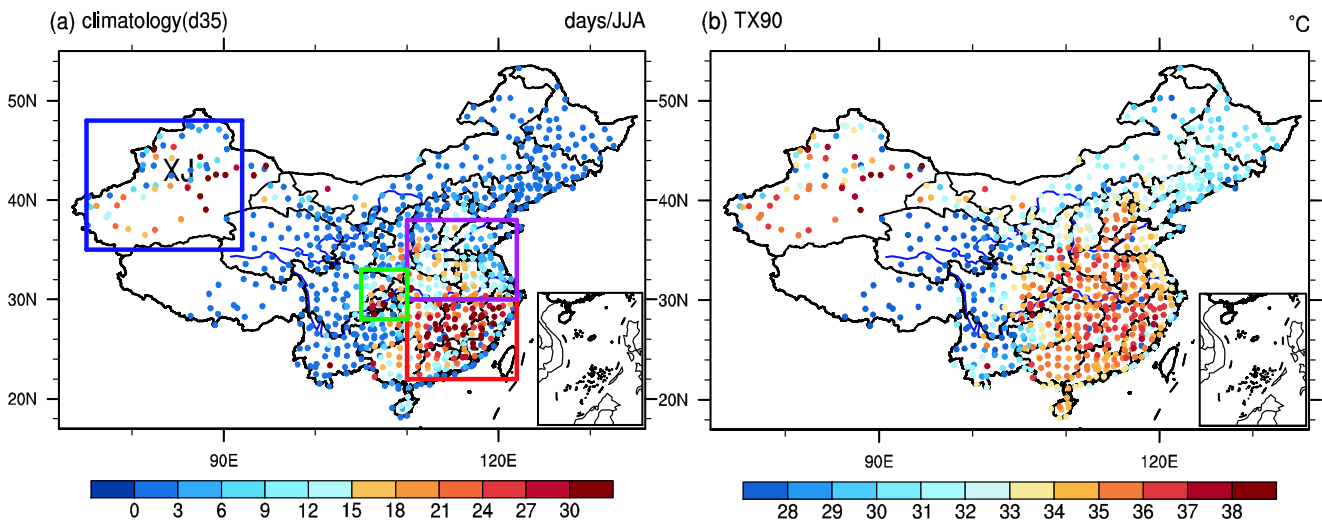


Fig. 2 Climatology of the NHD based on absolute index over China during 1960–2013 (a), the *blue box* represents Xinjiang region, the *green box* represents Chuanyu region, the *purple box* represents

Huanghuai region, the *red box* represents Southeast region; distribution of 90th percentile values of daily maximum temperature during 1960–1989 over China (b)

with the results of the NHD. The first two EOF modes explain about 23.9 % and 9.1 % of the total variances for the FHW based on absolute index, and 19.6 % and 12.9 % for the FHW based on percentile index.

For the FHW based on absolute index, the EOF1 and PC1 indicate an increase over north of Xinjiang, but a decrease over most regions of China, especially over southeast China, from 1960 to late 1990s. The trends reversed in these areas during the late 1990s to 2013. The EOF2 and PC2 reveal that the FHW increases (decreases) in Huanghuai area and west Xinjiang (south China) during the 1960s to 1970s and the late 1990s. The trends reversed in these areas during 1980s to early 1990s and 2000s.

For the FHW based on percentile index, the EOF1 and PC1 indicate a decrease over China during 1960 to the late 1990s

and an increase during the late 1990s to 2013. The EOF2 and corresponding PC2 reveal a decrease in north China (north of 35° N) during 1960 to 1995, but an increase in south China (south of 35° N). The trends reversed in these areas during 1995 to 2013.

3.2.2 Linear trend

According to the climatology and EOF modes of the NHD and the FHW, four sub-regions are chosen: Xinjiang region (75–92° E, 35–48° N), Huanghuai region (110–122° E, 30–38° N), Southeast region (110–122° E, 22–30° N), Chuanyu region (105–110° E, 28–33° N). The scopes of the four sub-regions are depicted in Fig. 2a. The four sub-regions are the regions where extreme temperatures frequently occur

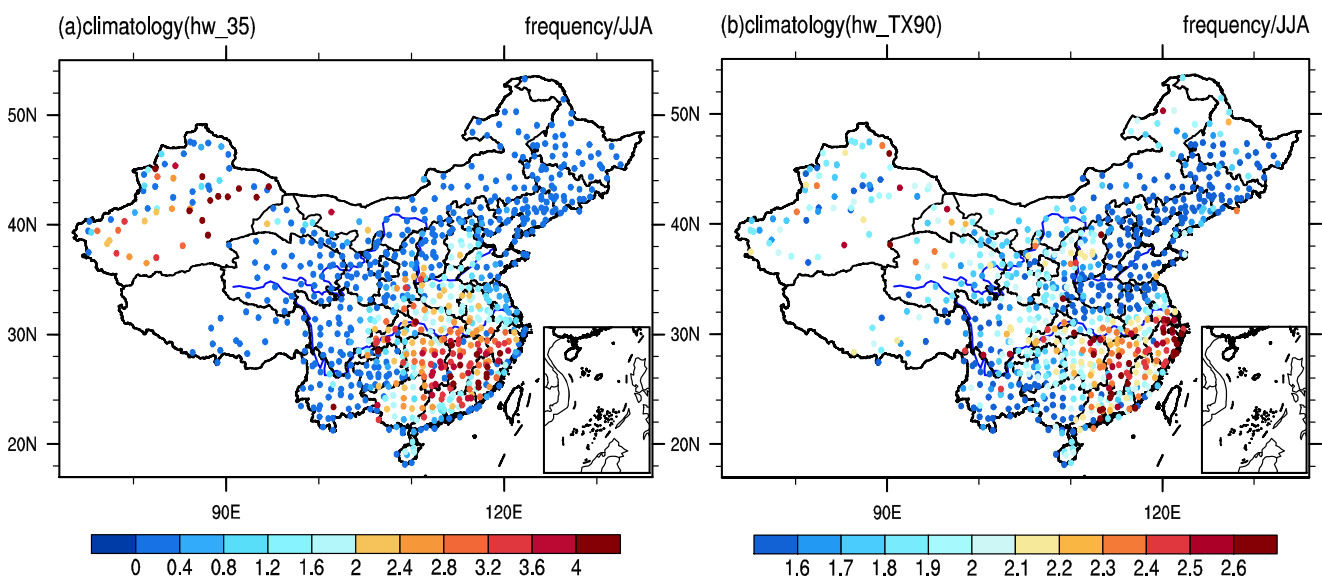


Fig. 3 Climatology of the FHW (frequency/JJA) based on absolute index (a) and percentile index (b)

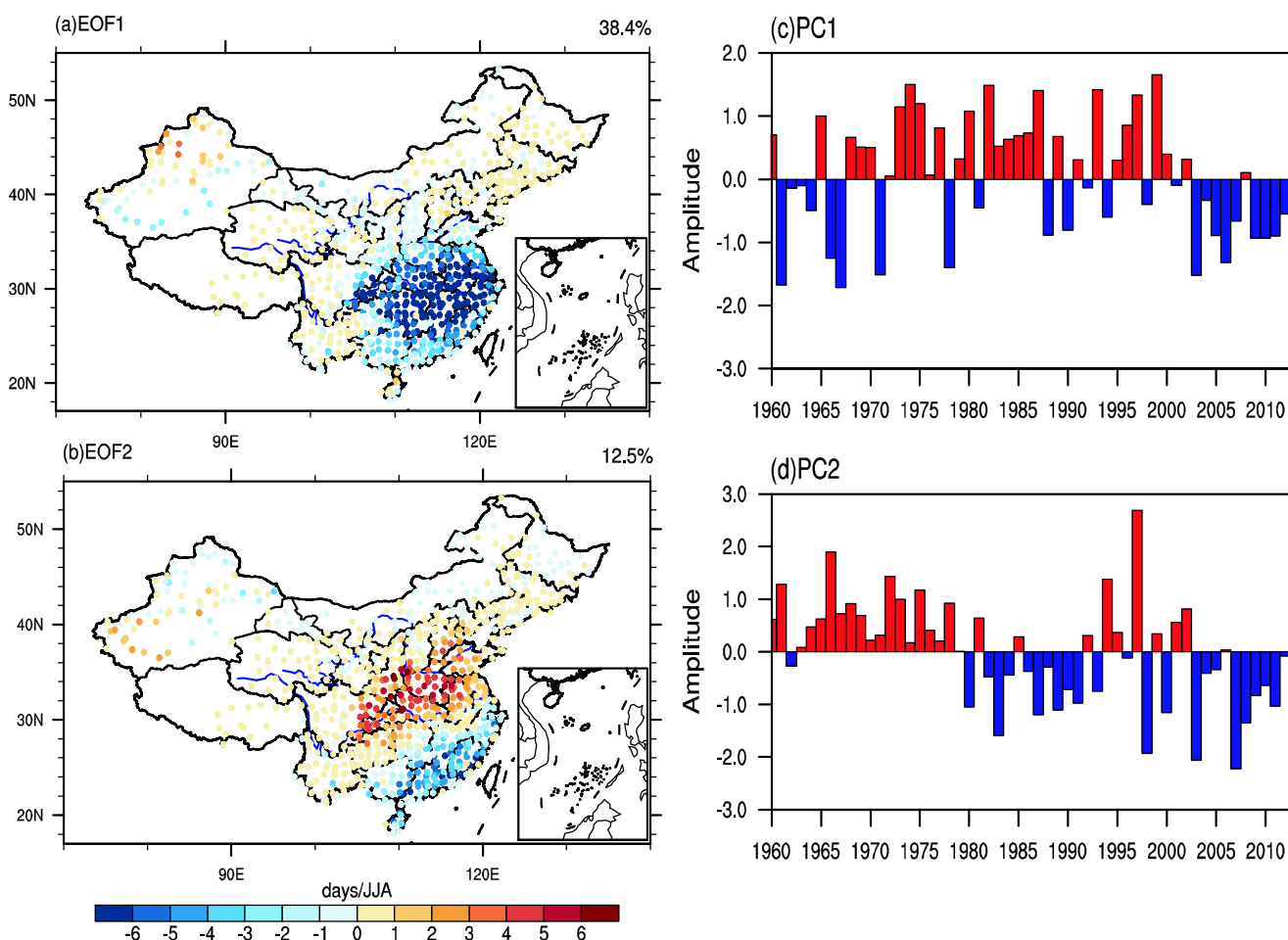


Fig. 4 The first EOF mode (a) and the second EOF mode (b) of the NHD based on absolute index over China and the first principal components (c) and the second principal components (d) during 1960–2013

(including NHD and FHW) and have a significant variation in the EOF modes. The regional averaged NHD (the stations where the averaged NHD is less than 1 day had been removed) and FHW are denoted as regional NHD and regional FHW.

Figure 6a displays the linear trend of the NHD based on absolute index over China during 1960–2013. The NHD increased in most part of China during 1960–2013, especially over Xinjiang and south of the Yangtze river, and most of the stations exceed the 95 % significance level. A decreasing trend is identified in Henan and Shandong province, but the change trend is not obvious as the trends at most of the stations do not exceed the 95 % significance level.

Figure 6b is the same as Fig. 6a but for the NHD based on percentile index. The NHD increased over most of China during 1960–2013. Compared with linear trend of the NHD based on absolute index, the increasing tendency based on percentile index is larger and the increasing areas are more scattered. A decreasing trend is also identified in Henan and Shandong provinces; however, the trends over most of the stations do not exceed the 95 % significance level.

Linear trends of FHW based on absolute index and percentile index over China during 1960–2013 (figures are omitted) are the same as those of NHD (Fig. 6). A decreasing trend is identified in Henan and Shandong provinces, but the trends over most of the stations do not exceed the 95 % significance level. The FHW increased during 1960–2013 in most regions, especially in south of the Yangtze river.

Table 2 shows linear trends of the NHD and FHW based on absolute index and percentile index in four sub-regions. The linear trends are more obvious for the NHD and FHW based on percentile index than based on absolute index. All regions exceed the 90 % significance level except Huanghuai area. The most significant linear trend exists in Southeast area, followed by Chuanyu area and then Xinjiang area. The linear trends of Southeast and Chuanyu areas are larger than national average, indicating that the NHD of these regions increased considerably. Based on the linear trends of the FHW in four sub-regions, the most significant linear trend appeared in Southeast area, followed by Xinjiang and Chuanyu areas.

Compared to the linear trend of the NHD and FHW based on absolute index (Ding et al. 2009), the pattern is almost

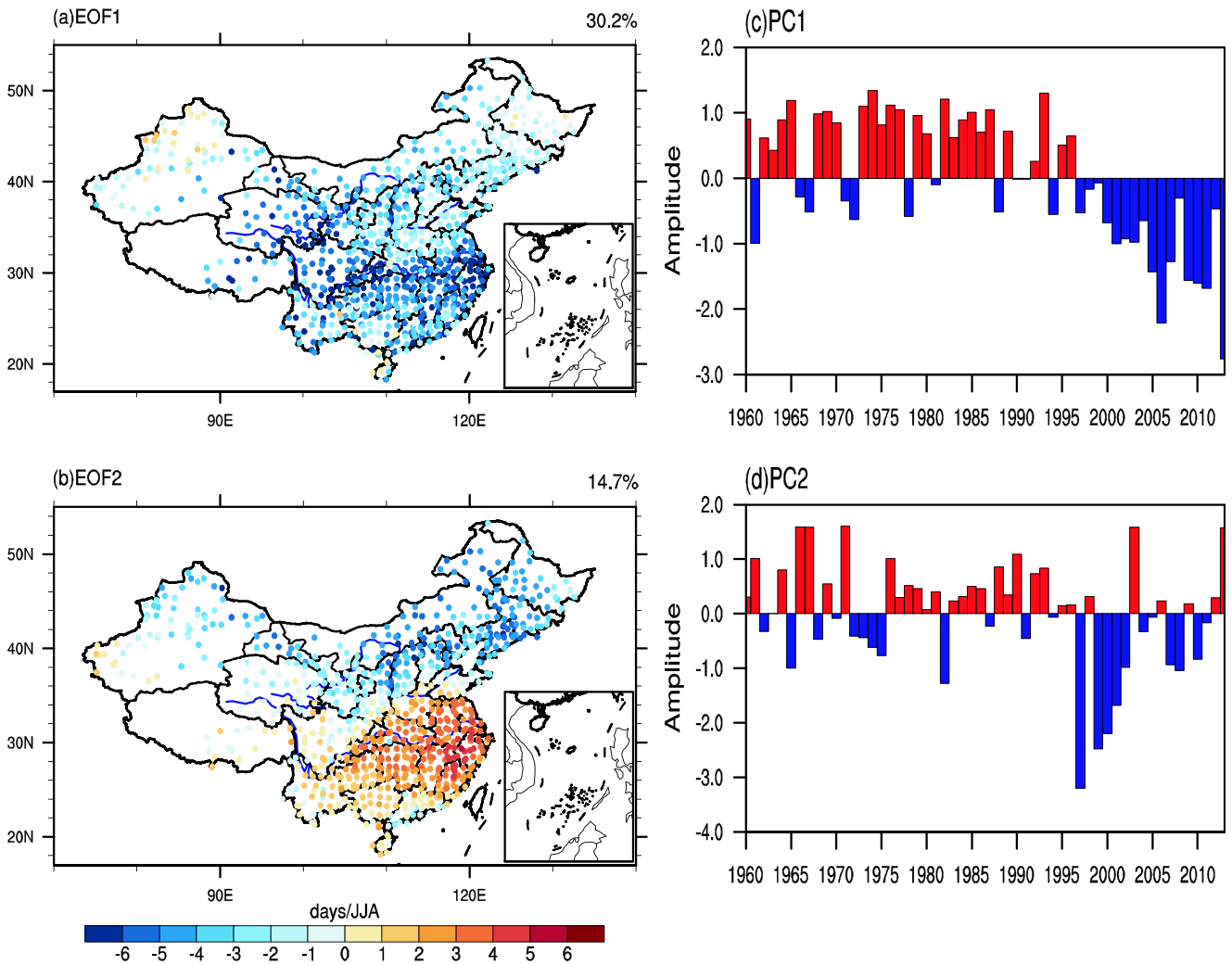


Fig. 5 The first EOF mode (a) and the second EOF mode (b) of the NHD based on percentile index over China and the first principal components (c) and the second principal components (d) during 1960–2013

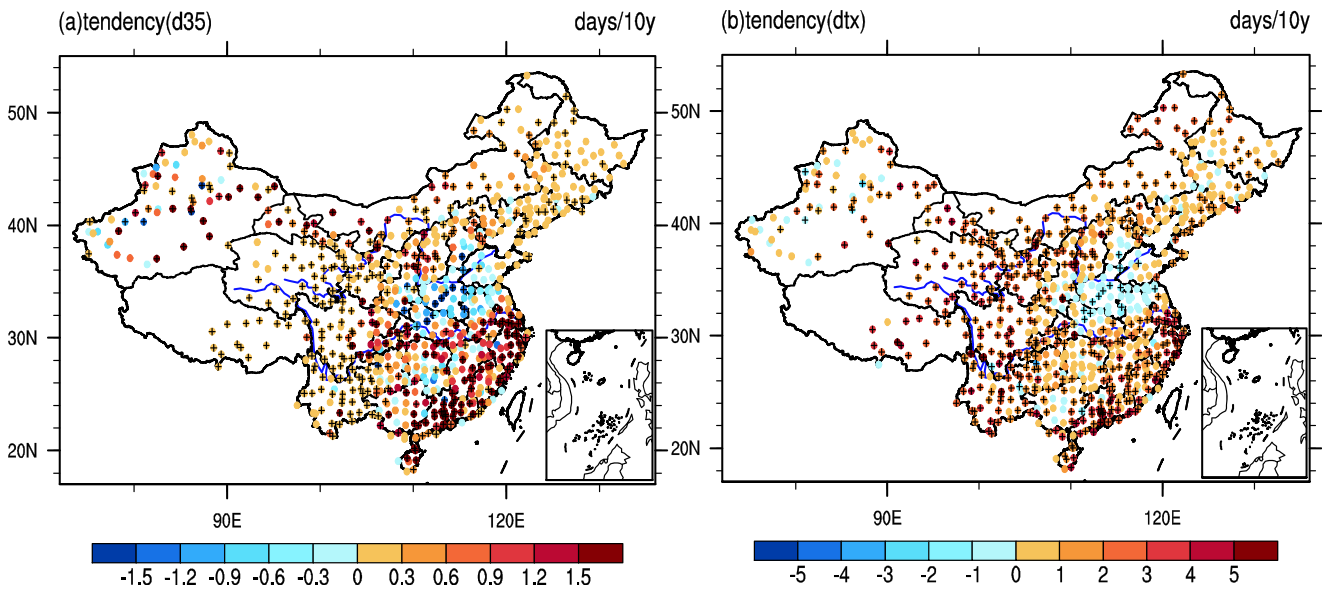


Fig. 6 Linear trend of the NHD based on absolute index (a) and percentile index (b) during 1960–2013 over China, the *plus signs* indicate station exceeds the 95 % significance level

Table 2 Linear trends of the regional NHD (day/decade) and FHW (frequency/decade) based on two indices over four sub-regions

Regions	NHD		FHW	
	Absolute index	Percentile index	Absolute index	Percentile index
National	0.05**	0.14**	0.07**	0.19**
Chuanyu	0.70*	1.80**	0.06	0.15**
Huanghuai	-0.04	0.30	-0.001	0.05
Southeast	1.20**	1.70**	0.21**	0.25**
Xinjiang	0.59**	0.92**	0.09**	0.14**

* represents exceeding the 90 % significance level

** represents exceeding the 95 % significance level

consistent, but the values of linear trend are smaller than the former research. For the linear trend of the NHD and FHW based on percentile index, both the pattern and value of the trends are basically consistent with the former research (Ding et al. 2009; Zhou and Ren 2011; Wang et al. 2012; Xu et al. 2013).

3.2.3 Inter-decadal variation

We use relative variations of the NHD and FHW every 10 years (the latter decade minus the former decade) to characterize the inter-decadal variation. Figure 7 indicates relative variations of the NHD based on absolute index every decade over China during 1961–2010. The changes of the NHD display obvious east-west characteristics during the 1960s to 1970s. Most stations in east China (east of 105° E) showed a significant decreasing trend, and an increasing trend is identified in west China (west of 105° E). From the 1970s to 1980s, the NHD reduced in north of the Yangtze river and increased in south of the Yangtze river. The most significant increasing trend occurred in Southeast China. In contrast, the NHD increased in north of the Yangtze river and decreased in south of the Yangtze river from the 1980s to 1990s. There is a consistent increasing trend of the NHD throughout the country from 1990s to 2000s, especially in south of the Yangtze river.

The relative variations of the NHD based on percentile index over China during 1961–2010 are showed in Fig. 8. Compared to the results based on absolute index (Fig. 7), the differences are located in the Tibetan Plateau (TP: Xizang, Qinghai) and Northeast China (NEC: Liaoning, Jilin, Heilongjiang). From the 1960s to 1970s, the NHD increased in the TP and NEC. The NHD had a decreasing tendency in the TP and an increasing tendency in the NEC from the 1970s to 1980s. From the 1980s to 1990s, most stations in the TP showed an increasing trend and a decreasing trend was identified in most stations of NEC. There is an increasing trend in the TP and NEC from the 1990s to 2000s. The relative variations of the NHD based on percentile index are more significant than those based on absolute index in the Tibetan Plateau and Northeast China. Inter-

decadal variations of the NHD in north China and TP regions are obvious based on percentile index.

Relative variations of the FHW based on absolute index and percentile index over China (figures are omitted) are consistent with the NHD, respectively (Figs. 7 and 8) during 1960–2013. Most stations in east China (east of 105° E) show a significant decreasing trend and an increasing trend is identified in west China (west of 105° E) from the 1960s to 1970s. From the 1970s to 1980s, the FHW reduced over north of the Yangtze river and increased over south of the Yangtze river. The most significant increasing trend occurred over Southeast China. In contrast, the FHW increased in north China and decreased in south China from the 1980s to 1990s. There is a consistent increasing trend of the FHW throughout the country from the 1990s to 2000s, especially in south of the Yangtze river. Therefore, the FHW has significant inter-decadal variation and regional characteristics.

We analyze the changes and inter-decadal variability of the four sub-regions through a 9-year sliding average. From the changes of regional NHD based on absolute index for four sub-regions during 1960–2013 (Fig. 9), it is found that all the four sub-regions exhibit inter-decadal variation. Figure 9a indicates that the NHD over Chuanyu area during 1960–2013 exhibits a variation of “increase-decrease-increase,” and the NHD decreased dramatically in the 1980s and then increased since the end of 1980s. The linear regression coefficient of the NHD over Huanghuai area was -0.04d/decade, which showed a slight reduction during 1960–2013. It can be concluded that the NHD reduced from the 1960s to 1980s and increased since 1990s over Huanghuai area (Fig. 9b). There is a tendency of “decrease-increase” in Southeast area (Fig. 9c). The NHD show a slight decreasing trend from the 1970s to 1990s and an increasing trend after the late 1990s, especially since 2000. Figure 9d indicates that the NHD displays a variation of “increase-decrease-increase” over Xinjiang (slight increase from the 1960s to 1980s, decrease during the 1980s to the late 1990s, and increases after

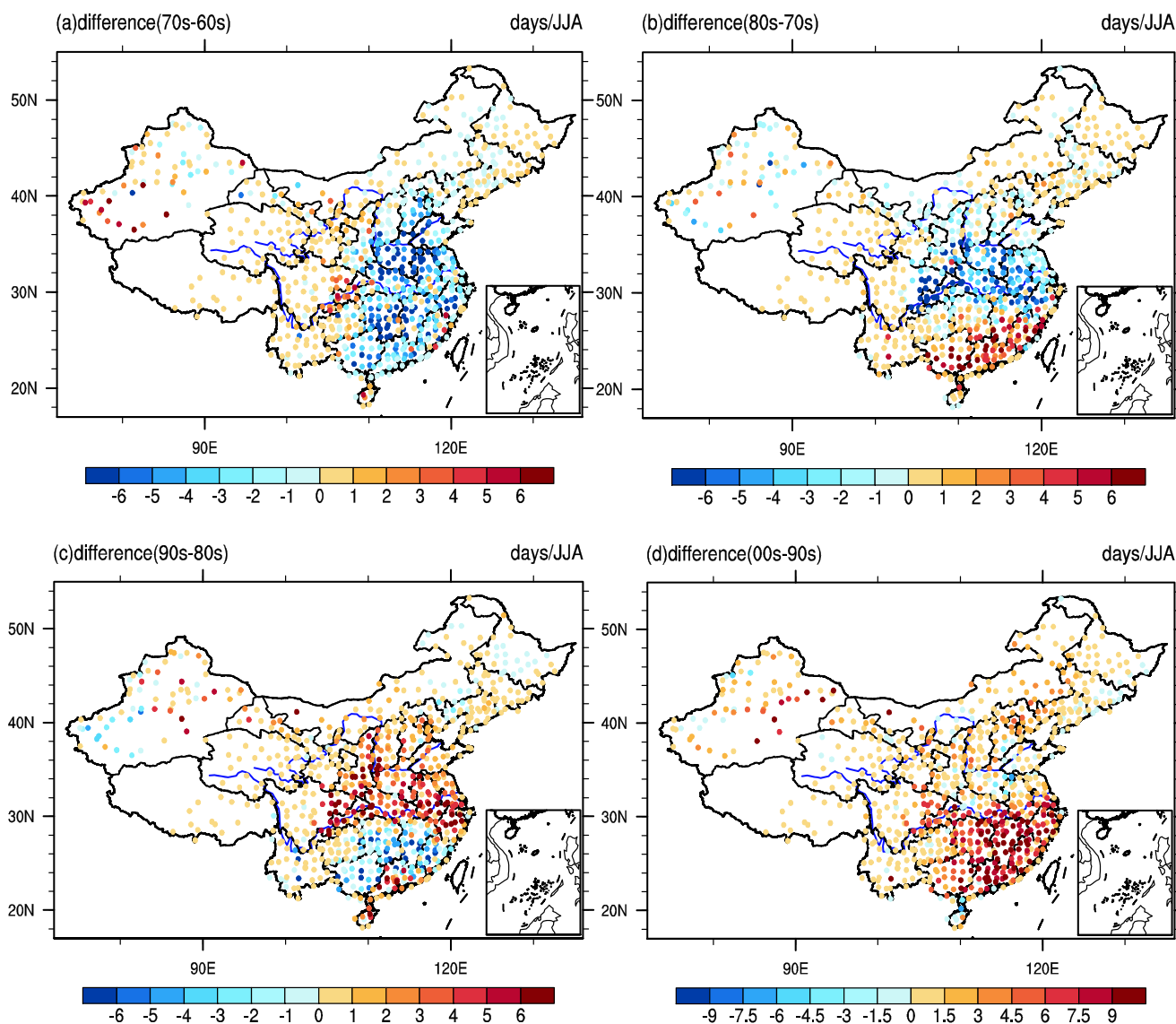


Fig. 7 Decadal variations of the summer averaged NHD based on absolute index during 1961–2010 over China. Difference of average NHD between 1971–1980 and 1961–1970 (a), between 1981–1990 and

1971–1980 (b), between 1991–2000 and 1981–1990 (c), between 2001–2010 and 1991–2000 (d)

the end of the 1990s). Changes of regional averaged NHD based on percentile index for sub-regions during 1961–2013 (figures are omitted) are consistent with those based on absolute index (Fig. 9).

Changes of regional averaged FHW based on absolute index and percentile index for four sub-regions during 1960–2013 (figures are omitted) are consistent with those based on the NHD (Fig. 9). The FHW of the four sub-regions increased rapidly since 1990s. It is found that all of the four sub-regions have the significant inter-decadal variation.

The results of trend and inter-decadal variation of the regional-averaged NHD and FHW are compared with the EOF modes. It is found that the linear trends for the sub-regions are basically consistent with the features of

EOF1 mode. Inter-decadal variations for the sub-regions are generally in accord with the results of EOF2 mode.

3.2.4 Abrupt shifts

Although the NHD and the FHW of the four sub-regions exhibit obvious inter-decadal variation, the abrupt shift is not clear. The Mann-Kendall method and 11-year sliding t -test are used to examine whether the four regional NHD and FHW exhibited sudden shifts during 1960–2013.

Mann-Kendall statistic curves of the regional NHD based on absolute index for four sub-regions during 1960–2013 are displayed in Fig. 10. The intersection points appeared in 1978 and 2000 over Chuanyu area (Fig. 10a), indicating that there were two sudden shifts

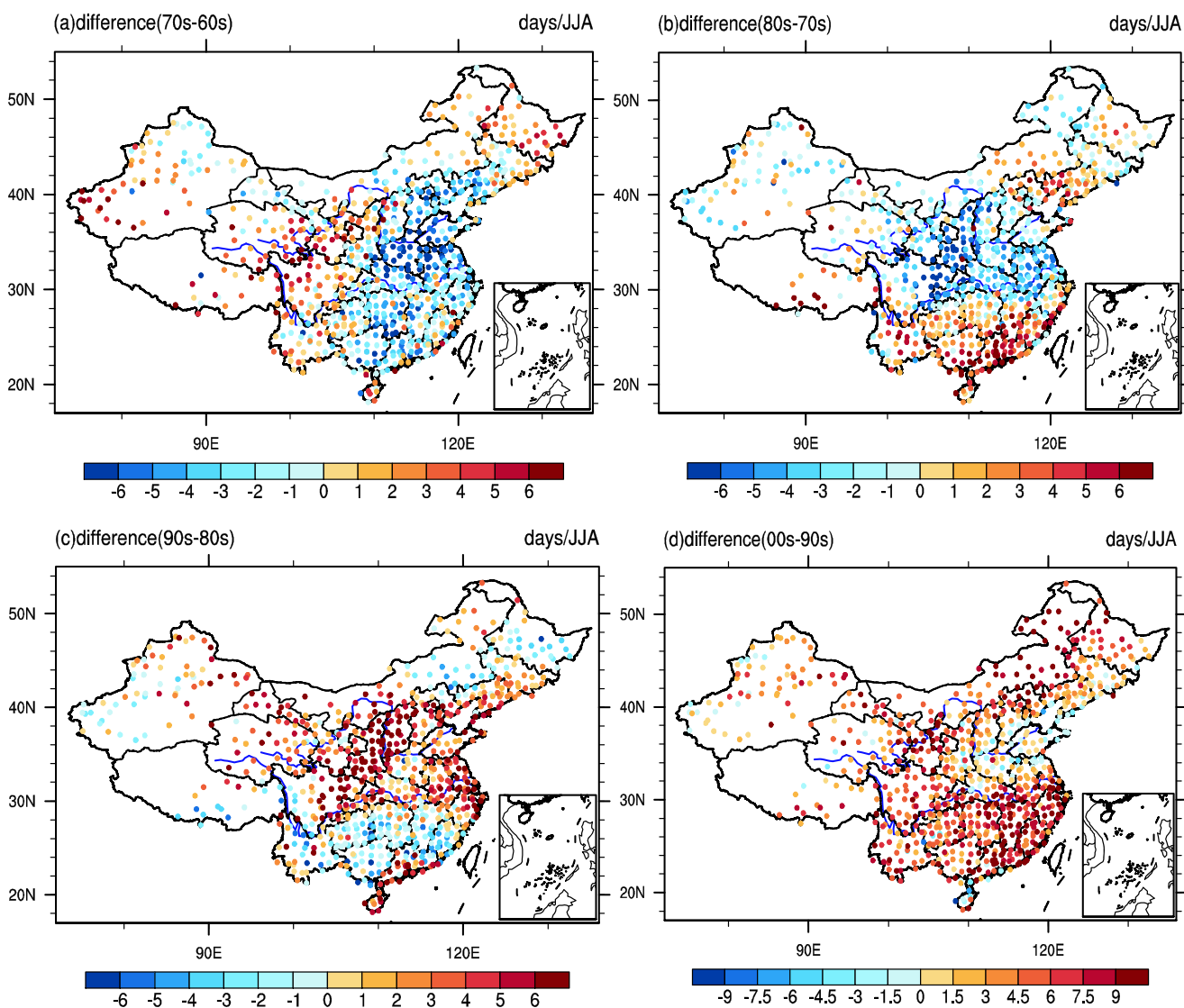


Fig. 8 Decadal variations of the summer averaged NHD based on percentile index during 1961–2010 over China. Difference of average NHD between 1971–1980 and 1961–1970 (a), between 1981–1990 and

1971–1980 (b), between 1991–2000 and 1981–1990 (c), between 2001–2010 and 1991–2000 (d)

(1978 and 2000) of regional NHD in recent 54 years. Figure 10b shows that abrupt shifts in Huanghuai area basically coincided with Chuanyu area, with sudden shifts in 1973 and 2000. Based on the results of Mann-Kendall method, it is found that a sudden shift of the regional NHD occurred in 2003 over Southeast area (Fig. 10c). However, no abrupt shift of the regional NHD in Xinjiang area is found in the recent 54 years (Fig. 10d).

Mann-Kendall statistic curves of the NHD based on percentile index for sub-regions during 1960–2013 (figures are omitted) are consistent with the curves based on absolute index (Fig. 10). Table 3 shows the years of abrupt shifts of the regional NHD and FHW based on absolute index and percentile index over the four sub-regions during 1960–2013. It is found that the years of

abrupt shifts of the regional NHD based on percentile index are 2–3 years earlier compared with those of the NHD based on absolute index.

The abrupt shifts of the regional FHW based on absolute index and percentile index during 1960–2013 (figures are omitted) are similar to those of the NHD. When the regional FHW is investigated based on absolute index, the two sudden shifts appeared in 1978 and 2000 over Chuanyu area in recent 54 years; abrupt shifts occurred over Huanghuai area in 1973 and 2000; one sudden shift occurred in 2000 over Southeast area; no abrupt shift of regional FHW is found over Xinjiang area in recent 54 years. Table 3 also indicated that the years of abrupt shifts of the regional FHW based on percentile index are 2–3 years earlier compared with those results based on absolute index.

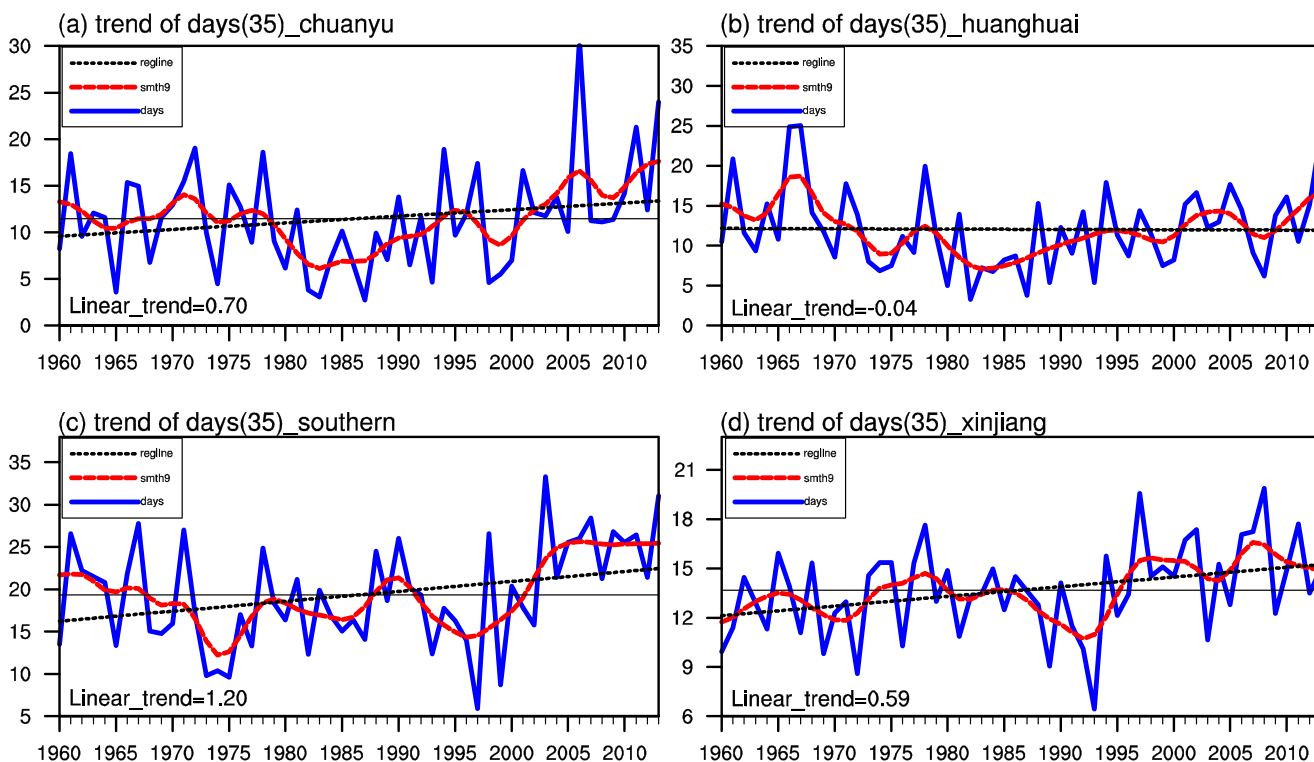


Fig. 9 Changes of the regional NHD based on absolute index during 1960–2013 for Chuanyu (a), Huanghuai (b), Southeast (c), and Xinjiang (d). The blue solid line depicts the number of heat days; the red dashed line depicts binomial 9a sliding average of regional NHD; the black dotted line depicts a linear trend; the black solid line depicts the average of regional NHD during 1960–2013

In addition, the 11-year sliding *t*-tests are performed on the above variation of the regional NHD and the regional FHW

over the four sub-regions; the results are consistent with those based on the Mann-Kendall method.

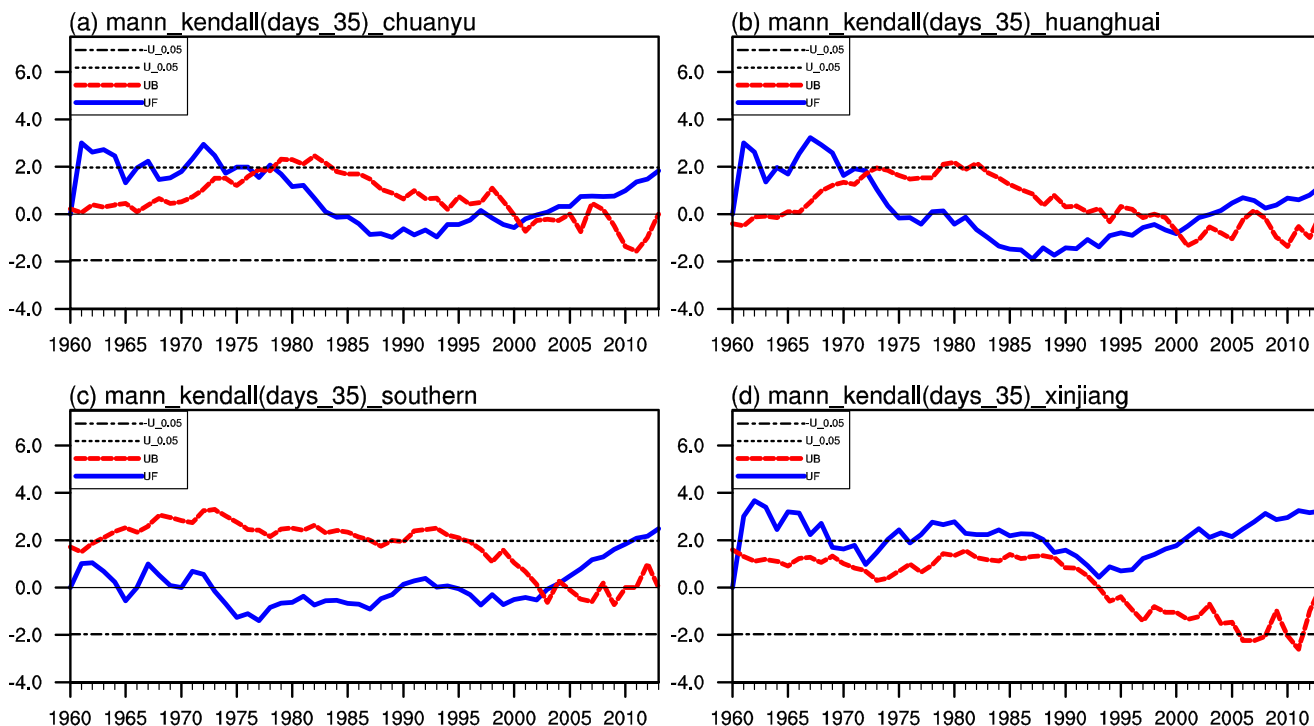


Fig. 10 Mann-Kendall statistic curves of the regional NHD based on absolute index for Chuanyu (a), Huanghuai (b), Southeast (c), and Xinjiang (d) during 1960–2013 (the blue line depicts UF, the red line depicts UB, the two black lines are the significance level of 0.05)

Table 3 Years of abrupt shifts of the regional NHD and FHW based on two indices over four sub-regions during 1960–2013

Regions	NHD		FHW	
	Absolute index	Percentile index	Absolute index	Percentile index
Chuanyu	1978, 2000	2000	1978, 2000	1976, 2000
Huanghuai	1973, 2000	1973, 1998	1973, 2000	1973, 1997
Southeast	2003	1999	2000	1999
Xinjiang	–	–	–	–

4 Discussion

In order to investigate the relationship between the two indices, we calculate the correlation coefficients over each station between the absolute index and the percentile index for the NHD and the FHW during 1960–2013. The national averaged coefficients over China are 0.76 and 0.58, respectively, both exceeding the 95 % significance level. Differences between the two indices for the NHD and the FHW mainly existed in west and north China. Because daily maximum temperatures over west and north China are generally below 35 °C, the quantitative values of the NHD and the FHW are tiny when the threshold is 35 °C. If using the percentile index, the spatial and temporal features for the NHD and the FHW are well displayed. Therefore, the percentile index is more reasonable than absolute index over China.

To demonstrate the relationship between the NHD and the FHW, we calculate the correlation coefficients over each station between the NHD and the FHW for the absolute index and the percentile index during 1960–2013. The national averaged coefficients over China are 0.77 and 0.78, respectively, exceeding the 95 % significance level, indicating that the NHD and the FHW are well associated. The results of the EOF analysis show that the explained variance of the FHW is smaller than the NHD, indicating that the spatial and temporal features of the FHW are more complicated. Heat wave as a continuous extreme temperature event, the occurrence mechanism, and sustaining mechanism are complicated.

Comparing with recent researches which focus on climatology and tendency of a hot day and heat wave (Ding et al. 2009; Zhou and Ren 2011; Xu et al. 2013), our results are generally consistent with the researches. For the decadal variations of NHD based on the two indices (Figs. 7 and 8), the conclusions found in our manuscript are consistent with former researches (Shi et al. 2009; Sun et al. 2011). Our results are more comprehensive because the updated temperature data from more stations and length are used. Qi and Wang (2012) found that extreme heat days exhibit an abrupt shift in the early 1990s for the average of whole China, but our manuscript indicated that abrupt shifts occurred in 1970s and around 2000 for the four sub-regions; the differences may be attributed to updated dataset and significant regional characteristic.

Under the background of global warming, the cooling trend is identified in east-central China. From the decadal variations (Figs. 7 and 8) and the changes of regional NHD for Huanghuai area (Fig. 9b), we found that the cooling trend in east-central mainly occurred before 1990. The possible mechanisms for this unexpectedly cooling trend include two major aspects. One possible reason is the increasing of atmospheric aerosols. Most aerosols reflect sunlight to space and have a global cooling effect (Penner et al. 2004). Therefore, it may contribute to a decreasing tendency of extreme temperature. Yu et al. (2004) and Yu and Zhou (2007) indicated that the cooling trend in central China may be connected to stratospheric temperature changes and involves interaction between the troposphere and stratosphere. Model simulations suggested a significant contribution by sulfate aerosols to the cooling, which induces a positive gradient of air temperature in the middle-upper troposphere and an enhanced East Asian summer monsoon, leading to more clouds over central China (Li et al. 2007).

Present investigation found that under global warming, the NHD and the FHW exhibit significant inter-decadal variation with obvious regional features. There are numerous factors responsible for the spatial and temporal features of extreme temperature events, such as atmospheric circulation, sea-air interaction, and land surface. Further studies are needed to explore the mechanism of the spatial and temporal features of extreme temperature events.

5 Summary

Based on daily air temperature data from 772 stations over China, present study adopts absolute index and percentile index to investigate the spatial and temporal features of summer extreme temperature over China during the period of 1960–2013. Xinjiang and southeastern China are two major domains where heat days and heat waves frequently occur. The NHD and the FHW have a consistent increasing trend throughout the country except for Shandong and Henan provinces where a decreasing trend is identified. Compared with the trend of the NHD and the FHW based on absolute index, there is a larger tendency of increasing for the NHD and the FHW based

on percentile index and the distribution of great increasing areas are more scattered with strong regional characteristics.

For the NHD and the FHW based on absolute index, the most significant feature, revealed by EOF1 and PC1, is that the NHD and the FHW decreased over south China during 1960 to late 1990s and increases during the late 1990s to 2013. The EOF2 and PC2 display a decadal variability with 10a period, indicating an opposite anomaly between Huanghuai area and south China. For the NHD and the FHW based on percentile index, the most prominent feature revealed by EOF1 and PC1 is a uniform variation over China, with a decrease over China during 1960 to late 1990s, and an increase during the late 1990s to 2013. EOF2 and PC2 reveal that the NHD and the FHW decreased in north China during 1960 to 1995, but increased in south China; the trends reversed in these areas during 1995 to 2013.

Both the NHD and the FHW display significant inter-decadal variations over China. Although the changes for four regions (Xinjiang, Huanghuai, Chuanyu, and Southeast) displayed differences, the NHD and the FHW for all regions increased significantly after mid-1990s. Based on the Mann-Kendall method and 11-year sliding t test, Chuanyu had abrupt shifts in 1978 and 2000; Huanghuai had sudden shifts in 1973 and 2000; southeast China had an abrupt shift in the late 1990s; Xinjiang had no sudden shift during 1960–2013. The years of abrupt shifts of the regional NHD and the regional FHW based on percentile index are generally 2–3 years earlier compared with those based on absolute index.

Acknowledgments The authors thank the National Climate Center of the China Meteorological Administration for providing the meteorological data for this study. This work is supported by the National Basic Research Program of China (2012CB955604), the Strategic Priority Research Program of the Chinese Academy of Sciences (XDA05090402), the National Natural Science Foundation of China (41275083 and 91337105), and the National Outstanding Youth Science Fund Projection of China (41425019).

References

- Alexander LV et al. (2006) Global observed changes in daily climate extremes of temperature and precipitation. *J Geophys Res-Atmos* 111 doi:10.1029/2005jd006290
- Chen HB, Fan XH (2007) Some extreme events of weather, climate and related phenomena in 2006. *Clim Environ Res* 12:100–112
- Chen HB, Fan XH (2008) Some extreme events of weather, climate and related phenomena in 2007. *Clim Environ Res* 13:102–112
- China Meteorological Administration (CMA) (1979) The rules of surface meteorological observation. The Meteorological Press, Beijing, p. P186
- Choi G et al. (2009) Changes in means and extreme events of temperature and precipitation in the Asia-Pacific Network region, 1955–2007. *Int J Climatol* 29:1906–1925. doi:10.1002/joc.1979
- Ding T, Qian W, Yan Z (2009) Changes in hot days and heat waves in China during 1961–2007. *Int J Climatol* 30:1452–1462. doi:10.1002/joc.1989
- Dole R et al. (2011) Was there a basis for anticipating the 2010 Russian heat wave? *Geophys Res Lett* 38. doi:10.1029/2010gl046582
- Easterling DR et al. (2000) Climate extremes: observations, modeling, and impacts. *Science* 289:2068–2074. doi:10.1126/science.289.5487.2068
- Frich P et al. (2002) Observed coherent changes in climatic extremes during the second half of the twentieth century. *Clim Res* 19:193–212. doi:10.3354/cr019193
- Hartmann et al. (2013) Observations: atmosphere and surface. In: Climate change 2013: the physical science basis. Contribution of working group I to the Fifth Assessment Report of the Intergovernmental Panel on Climate Change. Cambridge University Press, Cambridge, 208–222
- Luterbacher J et al. (2004) European seasonal and annual temperature variability, trends, and extremes since 1500. *Science* 303:1499–1503. doi:10.1126/science.1093877
- Li LJ, Wang B, Zhou TJ (2007) Contributions of natural and anthropogenic forcings to the summer cooling over eastern China: an AGCM study. *Geophys Res Lett* 34:L18807. doi:10.1029/2007GL030541
- Li QX et al. (2004) Detecting and adjusting temporal inhomogeneity in Chinese mean surface air temperature data. *Adv Atmos Sci* 21:260–268
- Li QX et al. (2009) A mainland China homogenized historical temperature dataset of 1951–2004. *Am Meteorol Soc* 90:1062–1065
- Manton MJ et al. (2001) Trends in extreme daily rainfall and temperature in Southeast Asia and the South Pacific: 1961–1998. *Int J Climatol* 21:269–284. doi:10.1002/joc.610
- Meehl GA, Tebaldi C (2004) More intense, more frequent, and longer lasting heat waves in the 21st century. *Science* 305:994–997. doi:10.1126/science.1098704
- Peng JB (2014) An investigation of the formation of the heat wave in Southeast China in summer 2013 and the relevant abnormal subtropical high activities. *Atmos Ocean Sci Lett* 7:286–290
- Penner JE, Dong XQ, Chen Y (2004) Observational evidence of a change in radiative forcing due to the indirect aerosol effect. *Nature* 427:231–234
- Qi L, Wang Y (2012) Changes in the observed trends in extreme temperatures over China around 1990. *J Clim* 25:5208–5222. doi:10.1175/jcli-d-11-00437.1
- Ren FM, Zhai PM (1998) Study on changes of China's extreme temperatures during 1951–1990. *Scintia Atmospherica Sinica* 22:217–217
- Ren GY et al. (2005) Recent progresses in studies of regional temperature changes in China. *Clim Environ Res* 10:701–716
- Rummukainen M (2013) Climate change: changing means and changing extremes. *Clim Chang* 121:3–13. doi:10.1007/s10584-013-0888-z
- Shi J, Ding YH, Cui LL (2009) Climatic characteristics of extreme maximum temperature in East China and its causes. *Chin J Atmos Sci* 33:347–358
- Solomon S et al. (2007) Climate change 2007: The physical science basis. Contribution of working group I to the Fourth Assessment Report of the Intergovernmental Panel on Climate Change. Cambridge University Press, Cambridge, p. 996
- Sun JQ, Wang HJ, Yuan W (2011) Decadal variability of the extreme hot event in China and its association with atmospheric circulations. *Clim Environ Res* 16:199–208
- Sun Y et al. (2014) Rapid increase in the risk of extreme summer heat in Eastern China. *Nat Clim Chang* 4:1082–1085. doi:10.1038/nclimate2410
- Tang HY et al. (2005) On change in mean maximum temperature, minimum temperature and diurnal range in China during 1951–2002. *Clim Environ Res* 10:728–735
- Wang ZY et al. (2012) Changing trends of daily temperature extremes with different intensities in China. *Acta Meteor Sinica* 26:399–409. doi:10.1007/s13351-012-0401-z
- Xu WH et al. (2013) Homogenization of Chinese daily surface air temperatures and analysis of trends in the extreme temperature

- indices. *J Geophys Res Atmos* 118:9708–9720. doi:[10.1002/jgrd.50791](https://doi.org/10.1002/jgrd.50791)
- Yang H, Li CY (2005) Diagnostic study of serious high temperature over south China in 2003 summer. *Clim Environ Res* 10:80–85
- Yu RC, Wang B, Zhou TJ (2004) Tropospheric cooling and summer monsoon weakening trend over East Asia. *Geophys Res Lett* 31: L22212. doi:[10.1029/2004GL021270](https://doi.org/10.1029/2004GL021270)
- Yu RC, Zhou TJ (2007) Seasonality and three-dimensional structure of interdecadal change in the East Asian Monsoon. *J Clim* 20:5344–5355
- Yan ZW, Yang C (2000) Geographic pattern of extreme climate changes in China during 1951–1997. *Clim Environ Res* 5: 267–267
- Zhai PM, Ren FM (1997) On changes of China's maximum and minimum temperatures in the recent 40 years. *Acta Meteorol Sin* 55:418–418
- Zhai PM, Pan XH (2003) Trends in temperature extremes during 1951–1999 in China. *Geophys Res Lett* 30. doi:[10.1029/2003gl018004](https://doi.org/10.1029/2003gl018004)
- Zhang DQ, Qian ZH (2008) Analysis of extreme events in China's temperature in recent 50 years using detecting method based on median. *Acta Phys Sin* 57:4634–4640
- Zhang N, Sun ZB, Zeng G (2008) Change of extreme temperatures in China during 1955–2005. *J Nanjing Inst Meteorol* 31:123–128
- Zhou YQ, Ren GY (2011) Change in extreme temperature event frequency over mainland China, 1961–2008. *Clim Res* 50:125–139. doi:[10.3354/cr01053](https://doi.org/10.3354/cr01053)